

Lawrence Berkeley National Laboratory

Recent Work

Title

COUPLED CHANNEL ALPHA DECAY THEORY FOR ODD-MASS NUCLEI, ^{253}es AND ^{255}Fm

Permalink

<https://escholarship.org/uc/item/2rs94814>

Author

Soinski, A.J.

Publication Date

1977-05-01

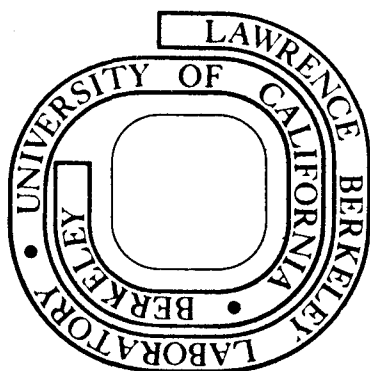
COUPLED CHANNEL ALPHA DECAY THEORY FOR
ODD-MASS NUCLEI, ^{253}Es AND ^{255}Fm

A. J. Soinski, J. O. Rasmussen,
E. A. Rauscher, and D. G. Raich

May 1977

Prepared for the U. S. Energy Research and
Development Administration under Contract W-7405-ENG-48

For Reference
Not to be taken from this room



LBL-6516
c.1

DISCLAIMER

This document was prepared as an account of work sponsored by the United States Government. While this document is believed to contain correct information, neither the United States Government nor any agency thereof, nor the Regents of the University of California, nor any of their employees, makes any warranty, express or implied, or assumes any legal responsibility for the accuracy, completeness, or usefulness of any information, apparatus, product, or process disclosed, or represents that its use would not infringe privately owned rights. Reference herein to any specific commercial product, process, or service by its trade name, trademark, manufacturer, or otherwise, does not necessarily constitute or imply its endorsement, recommendation, or favoring by the United States Government or any agency thereof, or the Regents of the University of California. The views and opinions of authors expressed herein do not necessarily state or reflect those of the United States Government or any agency thereof or the Regents of the University of California.

Coupled Channel Alpha Decay

Theory for Odd-mass Nuclei, ^{253}Es and $^{255}\text{Fm}^*$

A.J. Soinski**, J.O. Rasmussen

E.A. Rauscher, and D.G. Raich***

Nuclear Science Division, Lawrence Berkeley Laboratory

Berkeley, California 94720

*This work was supported by the U.S. Energy Research
and Development Administration

**Present Address: LFE Environmental Analysis Laboratories,
Richmond, CA - 94804

***Present Address: Chemistry Division, Argonne National
Laboratory, Argonne, Illinois 60439

ABSTRACT

An exact numerical coupled-channel integration treatment has been applied to the alpha decay of odd-mass spheroidal nuclei. The only non-central coupling of importance between an emitted alpha particle and rotational final states in the daughter nucleus involves the intrinsic quadrupole moment of the daughter. The nuclei ^{253}Es and ^{255}Fm are ideal cases to examine since alpha transitions to the favored bands are well known and angular distribution data from low temperature nuclear alignment is available.

We examined in detail two commonly used approximations; first, that near the nuclear surface there is zero projection of orbital angular momentum of favored alpha waves along the cylindrical symmetry axis of the daughter nucleus and second, that the intensity of each alpha-particle ℓ -wave is proportional to the product of a squared Clebsch-Gordan coefficient (times) the (calculated) spherical barrier penetrability factor. It is found that neither approximation holds within experimental error, and $M_\ell \neq 0$ alpha wave components must be introduced at the nuclear surface to give agreement with experimental intensities for both $\ell = 2$ and $\ell = 4$ waves.

Coupled Channel Alpha Decay
Theory for Odd-mass Nuclei, ^{253}Es and $^{255}\text{Fm}^*$

A. J. Soinski**, J. O. Rasmussen,

E. A. Rauscher and D. G. Raich***

I. Introduction

When a spheroidal nucleus undergoes decay, the noncentral electromagnetic field permits exchange of energy between internal nuclear excitation and the external alpha particle. The noncentral couplings of greatest importance involve collectively enhanced rotational E2 transitions in deformed nuclei. Starting with boundary conditions set at the spheroidal nuclear surface, the formal problem involves propagation of the alpha particle wave function outward through the anisotropic barrier to some distance where coupling effects are negligible.

Although other researchers have performed the numerical integration of coupled channel equations for the alpha decay of even-even spheroidal nuclei, there has been little analogous work on the alpha decay of odd-mass nuclei. In the latter case, an alpha particle wave of a given orbital angular momentum ℓ may branch to more than one energy level of the daughter nucleus. Thus, for the favored alpha decay of ^{233}U Chasman and Rasmussen¹ considered the decay of the s wave to the 5/2 level and the branching

of the d wave to the 5/2, 7/2 and 9/2 levels of ^{229}Th . Channel coupling effects are most significant for the case of a relatively weak wave, such as the highly hindered g wave, coupled to a strong wave such as the s wave. Therefore we have extended the work of Chasman and Rasmussen by considering the branching of the s, d and g waves in the favored alpha decays of both ^{253}Es and ^{255}Fm . Favored alpha decays are those decays in which the quantum numbers of the odd nucleon are the same for both the parent and daughter.

The nuclei ^{253}Es and ^{255}Fm , both spin 7/2 nuclei, are ideal cases for applying an exact numerical treatment because alpha transitions to the favored bands of the daughters have been well studied,² and angular distribution data from low temperature nuclear alignment experiments are available.³ If we include the branching of the $\ell = 0, 2, \text{ and } 4$ partial waves, then nine coupled second-order differential equations must be solved for favored decays to the five lowest levels (7/2, 9/2, 11/2, 13/2, 15/2) of the daughter rotational band. The $\ell = 6$ contributions have been taken into account in an approximate way (appendix I).

The results of the numerical integration test two commonly used assumptions. The first is that near the nuclear surface the favored alpha waves have zero projection of orbital angular momentum along the cylindrical symmetry z-axis of the daughter nucleus. Subject to this $M_\ell = 0$ constraint, we wish to determine if the coupled channel treatment can reproduce both the angular

distribution data and the experimental relative intensities to the spin $7/2$, $9/2$, $11/2$, $13/2$, and $15/2$ states of the daughter. The second assumption to be tested is that the relative intensities of a given ℓ -wave are given by the square of a Clebsch-Gordan coefficient times the calculated spherical barrier penetrability for the alpha group (formula of Bohr, Fröman and Mottelson (BFM)).⁴ Experimental data show deviations from the BFM expression for favored decay. It is of great interest to determine whether a careful coupled channel treatment of the barrier penetration explains the deviations while retaining the first assumption above.

II. Mathematical Formalism and Numerical Results

The formalism for alpha decay in the presence of a non-central field is given by Perlman and Rasmussen.⁵ A multipole expansion is made for the Coulombic potential energy outside the nuclear surface. The zero-order term is the central Coulombic term.

The E2 interaction contributes the first important coupling term. For nuclei with large hexadecapole deformations, E4 coupling may also be important;^{6,7} however, both ^{249}Bk and ^{251}Cf have small hexadecapole deformation. Therefore the coupled differential equations in the radial separation variable can be written as⁸

$$\begin{aligned}
 u''_{I_d, \ell} - \frac{2M}{\hbar^2} \left(\frac{2Ze^2}{r} + \frac{\hbar^2 \ell(\ell+1)}{2Mr^2} - Q_{I_d} \right) u_{I_d, \ell} &= \sum_{I'_d, \ell'} K_{I_d \ell' d}^2 u_{I'_d, \ell'} \\
 &= \sum_{I'_d, \ell'} K_{I_d \ell' d}^2 u_{I'_d, \ell'} \quad (1)
 \end{aligned}$$

where I_d , ℓ are the total angular momentum of the daughter and of the alpha particle in a give decay channel, M is the reduced mass, Z is the charge of the daughter nucleus, Q_{I_d} is the effective Q value for the alpha particle with electron screening and daughter recoil energy corrections, and the $K_{I_d \ell}^2$ are matrix elements of the quadrupole coupling operator which is proportional to the product of the intrinsic nuclear quadrupole moment Q_0 of the daughter times $P_2(\cos \theta)$ divided by r^3 , where r is the radial separation variable. For ^{249}Bk the value for Q_0 was taken to be the same as that for the parent, ^{253}Es ; namely, 13.1b^9 . For ^{251}Cf and ^{255}Fm we used approximately the same value; namely, 13.0b .

Explicit expressions for the quadrupole coupling matrix element were given for alpha decay in ref. 5 and ref. 8 and for optical model scattering applications and decay, see refs. (10, 11).

The general solutions of the uncoupled differential equations can be written as $U_L(\eta, \rho) = G_L(\eta, \rho) + iF_L(\eta, \rho)$ where G_L and F_L are the irregular and regular Coulomb functions⁹ respectively. Solutions of the coupled differential equations approach the Coulomb functions asymptotically at large radius.

In general the phase of an oscillating coupled-channel solution in the far region will differ from the phase of the corresponding Coulomb function. This phase difference is referred to as the quadrupole phase shift, $\phi_{I_d \ell}$. Although phase

shifts do not affect intensity calculations, they do affect angular distributions through the interference terms between alpha wave components of differing ℓ going to the same final state I_d . For notational convenience we sometimes use the single index j or k in place of the pair (I_d, ℓ) , where $j = 1$ through 9 denote respectively, $(I_d, \ell) = (7/2, 0), (7/2, 2), (7/2, 4), (9/2, 2), (9/2, 4), (11/2, 2), (11/2, 4), (13/2, 4)$ and $(15/2, 4)$.

The set of nine second-order coupled differential equations can be transformed into a set of eighteen first-order coupled differential equations having eighteen linearly independent solutions or, equivalently, nine complex solutions. Because the physically meaningful solutions decrease exponentially going outward through the barrier, it is not possible to obtain stable solutions by outward numerical integration. Instead we use Coulomb functions as starting conditions at 150 fm, a radius sufficiently large that the coupling forces are small, and integrate inward. The solutions of interest then increase in the direction of integration and remain stable. For the k^{th} linearly independent set of solutions, we initialized the k^{th} function and its derivative with the value of the complex Coulomb function corresponding to that channel and the remaining channels are initialized to zero. We label the resulting linearly independent set of complex solutions as $u_{jk}(r) = g_{jk}(r) + if_{jk}(r)$, representing the j^{th} channel of the k^{th} linearly independent solution.

Any general solution of the coupled differential equations may be expressed as a linear combination of the solutions just described; that is, the general solution for the j^{th} channel may be written as

$$\Psi_j(r) = \sum_{k=1}^9 c_k u_{jk}(r) \quad (2)$$

where the coefficients $c_k = a_k + ib_k$ are complex numbers. Because an alpha particle is assumed to exist in a quasi-stationary state prior to emission, the imaginary part of each wave function Ψ_j must essentially vanish near the nuclear surface. Using nuclear model constraints, which will be discussed in the next section, values for the real parts of the wave functions at the nuclear surface can be obtained. Then the set of nine complex simultaneous equations, $\Psi_j(r)$, can be solved for the coefficients c_k .

The system of simultaneous equations is conveniently represented in the matrix equation

$$\underline{U} \underline{C} = \underline{\Psi} \quad (3)$$

where the matrix elements u_{jk} of the 9×9 complex matrix U are the amplitudes of the linearly independent solutions on or near the nuclear surface. The elements of the column vector \underline{C} are the unknown complex coefficients c_k , and the elements of the

column vector Ψ are the purely real nuclear model surface amplitudes. The problem is solved by inverting the \underline{U} matrix

$$\underline{c} = \underline{U}^{-1}\Psi \quad (4)$$

The intensity of a given partial wave is the product of the square of the wave function amplitude and the velocity which goes as $Q_\alpha^{1/2}$. From the c_k values thereby obtained, and in view of the starting conditions of the pure Coulomb functions, the relative alpha partial wave intensities \mathcal{I}_k are

$$\mathcal{I}_k = |c_k|^2 Q_\alpha^{1/2} = (a_k^2 + b_k^2) Q_\alpha^{1/2} \quad (5)$$

where Q_α is the alpha decay energy in that channel. The quadrupole phase shifts ϕ_k are

$$\phi_k = \arg c_k = \tan^{-1}(b_k/a_k) \quad (6)$$

The most general way to present the results of the numerical integration is as the complex matrix \underline{U}^{-1} (the inverse of the complex 9x9 matrix \underline{U}). The matrix elements of \underline{U} are the amplitudes of the linearly independent solutions on a spherical surface near the nucleus. These matrices reduce to unit matrices for vanishing nuclear quadrupole moment. Operation with either matrix on a vector representing boundary conditions on a sphere near the nuclear surface will yield partial wave amplitudes and quadrupole phase shifts at large distances. If boundary conditions

are fixed on the spheroidal nuclear surface, then a Fröman matrix can be used to transform them to boundary conditions on a sphere at 10 fm. The real and imaginary components of the 9x9 matrix U have been given in refs. 12 and 13.

III. Numerical Results

In the similar work of Rasmussen and Hansen¹⁴ on even-even ^{242}Cm favored alpha decay, the boundary conditions for the real part of the solutions could be imposed by demanding agreement with experimental relative transition intensities to the rotational levels in ^{238}Pu . Because of partial-wave branching in odd-mass nuclei, however, the relative intensity data are inadequate. In our present formulation, there are nine real solutions, so after normalization eight boundary conditions must be specified. The experimental data provide only four relative alpha intensities going to the five daughter levels, and there are no direct experimental measurements of the partial wave amplitudes or relative phases contributing to each alpha transitions. The low-temperature angular distribution data provide two experimental numbers, the coefficients of the $P_2(\cos \theta)$ and $P_4(\cos \theta)$ terms in the angular distribution function, but they do not uniquely determine relative partial wave amplitudes and phases.¹²

Because there are insufficient experimental data to completely fix the boundary conditions, nuclear model constraints are used as well. We use the fundamental assumption underlying the "leading

order intensity relationships" of the strong coupling model^{9,15} that near the nuclear surface the projection of any partial wave's angular momentum along the cylindrically-symmetric 3-axis of the daughter nucleus, m_ℓ , has a value of $K_d \pm K_p$ where K_d and K_p are the projections of the daughter and parent total nuclear angular momentum on the 3-axis. For $(K_d + K_p) > \ell$ only one value of m_ℓ is allowed; for favored alpha decay $m_\ell = 0$ and $K_d = K_p = K$. The condition of only $m_\ell = 0$ components on a sphere of radius R_0 near the nucleus provides six boundary conditions, tying together the components of a given ℓ -wave in proportion to Clebsch-Gordan coefficients. Bohr, Fröman, and Mottelson⁴ and Asaro *et al.*¹⁶ have, in some applications, constrained the relative s, d and g wave intensities to the average of nearest neighbor even-even nuclei, but such a constraint is not as fundamental as the $m_\ell = 0$ constraint. The remaining two boundary conditions are left as free parameters and are denoted by α_2 , the ratio of total d to s wave amplitude at R_0 , and α_4 , the ratio of total g to s wave amplitude at R_0 . Therefore the nine elements of the column vector wave function of eq. 4 at R_0 are given as follows:

$$\Psi_j(R_0) = \alpha_\ell \langle \ell I_p 0 K | I_d K \rangle \quad (7)$$

with the trivial normalization condition $\alpha_0 = 1$. The real part of the wave function decreases exponentially going outward through the barrier region and oscillates in the far region.

Having chosen these boundary conditions, the numerical integration of the coupled differential equations permits us to test two assumptions of the strong coupling model as usually

applied. The first is that near the nuclear surface only $m_\ell = 0$ alpha partial waves occur. Subject to this $m_\ell = 0$ constraint, we wish to determine if the coupled channel treatment can reproduce both the experimental relative intensities to the five lowest rotational levels of the daughter nucleus and the angular distribution data. This $m_\ell = 0$ condition is equivalent to Bohr and Mottelson's "leading-order intensity relations". The second assumption is the usual approximate treatment of anisotropic barrier penetrability, in which the relative intensity of an ℓ -wave to a given level is calculated as a Clebsch-Gordan coefficient squared times a spherical barrier penetrability factor for the alpha group. This approximation, originally due to BFM, is exact either when $m_\ell = 0$ or in the limits of infinite moment-of-inertia or vanishing nuclear quadrupole moment.

It is interesting to compare the BFM predictions with intensity data for favored decay in several odd-mass deformed nuclei. In Fig. 1 we have plotted the ratios of hindrance factors of second to first excited states. The hindrance factors are from the compilation of Ellis and Schmorak.¹⁷ If these alpha groups were purely $\ell = 2$, the ratio would, by the BFM intensity relations, equal the indicated ratio of squared Clebsch-Gordan coefficients. Actually the ratio points are lower limits for the desired $\ell = 2$ intensity ratio, since the small correction for $\ell = 4$ components would raise them.

Let us now consider for ^{253}Es and ^{255}Fm the determination of the two free parameters α_2 and α_4 . The value for α_2 is largely determined by the requirement that the alpha intensity to the $9/2+$ daughter level be reproduced, because this level receives the largest d-wave component. In general there are two values for α_2 , one positive and one negative, that give satisfactory agreement with experiment. The sign of the anisotropy in the alpha particle angular distributions for both ^{253}Es and ^{255}Fm requires that the s and d waves be in phase; that is, that they interfere constructively near the nuclear poles. Therefore only positive values for α_2 are acceptable.

In like manner the alpha intensity to the $13/2+$ level largely determines the value for α_4 . The phase of the g wave is less well determined by the angular distribution data, but the ^{253}Es angular distribution data and alpha decay systematics suggest that the g wave is out of phase. Therefore only negative values for α_4 are acceptable.

From microscopic theory using Nilsson functions the values of both α_2 and α_4 can be estimated. Poggenburg^{18,19} calculated partial wave amplitudes on a Nilsson coordinate surface to be 1.035, 0.309 and -0.376 respectively for the $\ell = 0, 2$ and 4 waves of ^{253}Es and 1.008, 0.361, and -0.387 for ^{255}Fm . Applying a Fröman matrix

of argument $B = 1.36$, which is approximately correct* for the transformation from the Nilsson surface to a sphere near the nuclear radius, we obtain $\alpha_0:\alpha_2:\alpha_4 = 1:0.81:-0.10$ for ^{253}Es and $1:0.85:-0.09$ for ^{255}Fm .

Using the U^{-1} matrix and eqs. (5) and (7) for the relative intensities, we applied a least-squares fitting procedure allowing the surface amplitude ratios of d to s (α_2) and g to s (α_4) waves to vary.

The values of α_2 and α_4 were obtained by minimizing the weighted root-mean-square logarithmic differences between the theoretical and experimental intensities. The weighting reflected the uncertainties in the experimental intensities. The best fits to the experimental intensities are obtained with $\alpha_0:\alpha_2:\alpha_4 = 1:0.8580:-0.0977$ for ^{253}Es and $\alpha_0:\alpha_2:\alpha_4 = 1:0.7918:-0.1794$ for ^{255}Fm . The agreement of these amplitude ratios with those above calculated from microscopic theory is reasonable.

*In the work of Poggenburg et al.¹⁸ it was determined that a Fröman matrix argument of $B = 0.9$ was optimum for propagating the Legendre expanded wave function on a Nilsson stretched coordinate surface out to a spherical surface outside the barrier. In coupled channel work of Rasmussen and Hansen¹⁴ on ^{242}Cm it was determined that the Fröman argument of $B = -0.455$ was appropriate for propagation from a sphere near the nucleus but just beyond the range of the nuclear potential out to a sphere at large distance. Since Fröman arguments are additive, we thus take the argument for propagation across the nuclear surface to be the difference $0.9 - (-.455) \approx 1.36$. We approximated the Fröman matrix by interpolation from Fröman's tables.

These fits are plotted in the left-hand bars of Figs. 2 and 3. The right-hand bars refer to calculations with the $m_\ell = 0$ constraint removed, and they will be discussed in Sec. IV. The nuclear orientation results do not explicitly enter the least-squares fitting, but because of them only the region of positive α_2 was searched.

The logarithmic histogram display is chosen to show the predicted ℓ -mix within various alpha groups, but one should not be misled by the apparent large $\ell = 4$ crosshatched area which results from using a logarithmic and not a linear scale.

The partial wave intensities, Coulomb phase shifts, and quadrupole phase shifts corresponding to the least-squares solutions are summarized in Tables I and II for ^{253}Es and ^{255}Fm , respectively.

The pure Coulomb phase shifts are given by⁹

$$\sigma_\ell = \arg \Gamma (\ell + 1 + i \eta) \quad (8)$$

We shall discuss primarily the ^{253}Es results; however, the general comments are applicable also to the ^{255}Fm results.

Examination of the best fits to the intensities for both ^{253}Es and ^{255}Fm reveals a systematic discrepancy. The experimental intensity ratio between the second and the first excited states in the rotational band of the daughter is significantly larger than predicted for both nuclei. These states are populated primarily by d waves, and no combination of initial $\ell = 0, 2, 4$ ratios

reproduces the experimental intensity ratio if the $m_\ell = 0$ constraint in the nuclear frame is maintained. This same systematic deviation from BFM theory has been noted for favored bands of many alpha emitters as was shown in Fig. 1, but it is only now clear that the coupled channel treatment does not remove the discrepancy. As a result, we conclude that some d-wave component with $m_\ell \neq 0$ must be included near the nucleus.

Table III compares $\ell = 4$ branching prediction of our coupled-channel theory with the BFM formula¹⁰ as applied by Poggenburg¹⁸ and by Asaro et al.¹⁶ Asaro et al. used a square-well model to calculate alpha penetrabilities, while Poggenburg used an optical model nuclear potential. It can be seen that our coupled channel results are very close to the earlier BFM approximation, thus confirming the theoretical validity of approximating alpha branching at infinity by the product of the barrier penetrability times the square of the appropriate Clebsch-Gordan coefficient. However, there is a regime of higher $\ell = 4$ wave hindrance where channel coupling results in deviations from the BFM branching approximation. In Fig. 4, $\ell = 4$ branching ratios are plotted as a function of α_4 with $\alpha_2 = 0.89$. The values at $\alpha_4 = -0.101$ are given in Table I. In the vicinity of $\alpha_4 = 0.2$ the hindrance factors are highest, and the deviations from the BFM branching approximation are substantial. But channel coupling does not affect the accuracy of the simple Clebsch-Gordan branching expressions for $\ell = 4$ until higher $\ell = 4$ hindrance factors are encountered than those in ^{253}Es or ^{255}Fm .

IV. Inclusion of $m_\ell \neq 0$ Favored Alpha Decay Components

We have shown that a careful coupled-channel barrier treatment does not correct the BFM formula deviations visible in Fig. 1, under the constraint that the surface alpha wave function contains only $m_\ell = 0$ components. The systematic deviation of hindrance factor ratios from Clebsch-Gordan coefficient ratios must be explained in terms of $m_\ell \neq 0$ admixtures.

Gamma vibrational phonon ($\ell = 2, m_\ell = 2$) admixtures into actinide element nuclear wave functions have been calculated by Soloviev and co-workers,^{21,22} but these admixtures seem too small to change the d-wave branching to the degree required to fit intensity patterns and nuclear orientation data.

There are insufficient data to completely determine all $m_\ell \neq 0$ amplitudes. In general, four experimental intensity ratios are known, and when $m_\ell = 0$, two adjustable parameters α_2 and α_4 are derived by a least-square fit. There are then only two remaining degrees of freedom. If we introduce $m_\ell \neq 0$ amplitudes in a formulation that has two or more adjustable parameters, the problem becomes completely determined or overdetermined, and a least-squares fitting procedure cannot be used to derive parameter values. We have therefore attempted to introduce $m_\ell \neq 0$ amplitudes in a formulation with only one new adjustable parameter.

We propose a one-parameter constraint for introduction of $m_\ell \neq 0$ components from consideration that the mass of the alpha particle is not negligible compared to that of the daughter nucleus. While the alpha particle is within the nucleus, it is part of the system of spheroidal symmetry with symmetric top

inertial properties. When the alpha particle leaves the surface suddenly, the principal axes of the core will be suddenly shifted by a tilt angle θ . We represent the nuclear core inertial system classically by mass distributed along the body-fixed symmetry z' axis, or a diatomic molecule model such that the moment-of-inertia has the experimental value J . We then consider the removal of alpha particle mass at the nuclear radius at a particular angle χ in the body fixed y - z plane. (Equivalently we may add alpha particle mass at $-\chi$.) The new principal inertial axes are rotated from the old by angle θ given by

$$\sin 2\theta = \frac{M_{\alpha} R^2}{J} \sin 2(\chi - \theta) \quad (9)$$

Since the mass 250 region $\frac{M_{\alpha} R^2}{J} \approx 0.11 \ll 1$, we can make a small θ approximation of the above tilt equation to give

$$\theta \approx \frac{M_{\alpha} R^2}{J} \sin 2\chi \left(1 + \frac{M_{\alpha} R^2}{J} \cos 2\chi\right)^{-1} \quad (10)$$

We think that the appropriate average alpha emission angle χ (in the nuclear frame) should refer to the alpha wave outside the barrier. Thus, we may roughly estimate $\langle \chi \rangle$ directly from hindrance factors of even-even neighbors. For nuclei with the maximum $\ell = 4$ hindrance factors ($A \sim 244$) we believe $\langle \chi \rangle$ to have the value of the first zero of $P_4(\cos \chi)$, namely $\sim 30^\circ$. The trend of hindrance factors is such that $\langle \chi \rangle$ is a monotonically increasing function of mass number throughout the actinide region, and at the highest masses for which alpha fine structure has been measured the rising $\ell = 2$ hindrance has not yet gone through a maximum. Hence, $\langle \chi \rangle < 55^\circ$, the zero of $P_2(\cos \chi)$. If we take

for $\langle \chi \rangle$ an approximate value for ^{253}Es and ^{255}Fm of $\approx 45^\circ$, we can solve eq. (9) to get

$$\tan 2\theta \approx 0.11$$

or

$$\theta \approx 0.05$$

Thus, we would take the favored alpha wave amplitude of $m_\ell = 0$ at the surface and rotate the coordinate system, generating $m_\ell \neq 0$ components in the new frame. In this scheme the $m_\ell = 0$ amplitudes, $A_{\ell 0}$ are transformed by the rotation matrices with Eulerian angles $(0, \theta, 0)$. Thus, the new amplitudes are given as

$$A'_{\ell m} = D_{0m}^\ell(0, \theta, 0)A_{\ell 0}$$

In our numerical studies we have in this way introduced amplitudes A'_2 , and A'_4 , with one new adjustable parameter θ .

With our numerical solutions of the coupled-channel equations we have made a weighted least-squares determination of the best values of α_2 , α_4 , and θ to fit the experimental intensities. The original two-parameter least-squares fits (i.e., with the constraint $\theta = 0$) for $m_\ell = 0$, were presented in Sec. III, and Figs. 2 and 3 there also show the fits with θ unconstrained.

The optimum α_2 , α_4 , and θ values are for ^{253}Es 0.891, -0.117, and .306 radians, respectively. The corresponding values for ^{255}Fm are 0.828, -0.250, and 0.0633. Our one additional parameter θ can be seen from Figs. 2 and 3 to have improved the 11/2:9/2 branching ratio ($\ell = 2$), and the least-squares θ values are in satisfactory agreement with the estimate of tilt of principal axes during alpha decay.

The 15/2:13/2 branching ratio ($\ell = 4$) is not in very good agreement with theory, but the weak $\ell = 4$ groups may be affected by our truncation of the coupled-channel equations to exclude $\ell \geq 6$.

In summary we conclude that the deviation of $\ell = 2$ favored alpha hindrance factor ratios from the leading-order Clebsch-Gordan intensity relations is due to a kind of recoil term in the core rotational inertial system. The effect is to introduce $m_\ell \neq 0$ components into the favored alpha wave function at the nuclear surface. Although we solved the nine coupled channel equations only for parent spin 7/2, we can reasonably infer a similar behavior for the several $I_i = 5/2$ cases plotted in Fig. 1. As the mass number increases the mean alpha emission angle $\langle \chi \rangle$ in the nuclear frame shifts from small values toward 45 or 50° for the mass 250 region, the deviations should monotonically increase, as they do for the spin 5/2 cases.

We have with the coupled channel equations calculated the quadrupole phase shifts, which affect the interference terms in angular distribution experiments involving favored alpha decay. It would be interesting to have experimental α - γ angular correlation studies to test our predicted angular momentum mixtures and phase shifts for decay to excited rotational band members. The low-temperature nuclear orientation experiments could not resolve individual alpha groups and were thus mainly sensitive to the composition of the alpha group to the band head.

Appendix I

Exclusion of $\ell = 6$ Partial Waves
From Coupled Differential Equations

In order to limit the number of coupled differential equations to be solved, the $\ell = 6$ and higher angular momentum waves were excluded from our analysis. The hindrance factor for the $\ell = 6$ wave of the nearest neighbor Cf isotope is approximately 1000, whereas the hindrance factor for the $\ell = 4$ wave is¹⁷ approximately 30. Therefore the $\ell = 6$ wave cannot noticeably affect the $\ell = 4$ branching. Because the $\ell = 6$ wave was excluded from the theoretical analysis, an approximate i-wave component was subtracted from the experimental intensities before making the comparison with theory. This was done as follows. Ahmad²³ has measured the alpha intensities to the $17/2+$ and $19/2+$ levels of ^{253}Es (see Table IV). These levels are populated by $\ell = 6$ and higher angular momentum waves only, and we assumed that the higher ℓ waves are much weaker than the i-wave. The $\ell = 6$ penetrability factor for alpha decay to the $17/2+$ level, which was obtained by extrapolating Poggenburg's¹⁸ penetrabilities, was multiplied by the appropriate squared Clebsch-Gordan coefficient in order to obtain a relative theoretical intensity which was normalized to Ahmad's experimental intensity. The process was then reversed to obtain the i-wave component to the lower spin states of the

favored rotational band. The results are given in Table IV.

For ^{255}Fm alpha decay the experimental intensity to the $17/2+$ level is unknown; therefore we assumed that Poggenburg's calculations correctly predict the relative i-wave component. We believe this approximation is permissible because the correction is, in any case, small, and the correction has a significant effect only on the $13/2+$ and $15/2+$ intensities, which already have small weighting factors in the fitting routine. While it is true that any error in this extrapolation from Poggenburg will to some degree be reflected in our fit of α_4 , our major fitting difficulty is in reproducing the ratio between the $9/2+$ and $11/2+$ intensities, which is not strongly affected by either α_4 or the correction. Our corrections to the ^{255}Fm experimental intensities are also given in Table IV.

The reliability of our i-wave correction for ^{255}Fm decay is indicated by applying the same method to ^{253}Es . The subtracted components would then be 0.0001, 0.0016, 0.0031, 0.0060 and 0.0033 for the $7/2+$ through $15/2+$ levels. The differences between these values and the ones given in Table IV suggest that the i-wave, like the d wave, may be more skewed toward the lower levels of the rotational band than the BFM branching relation predicts.

Appendix II

Accuracy of Computations

Several numerical tests on the computer programs were performed. The regular and irregular Coulomb functions were integrated inward from 150 fm to 10 fm with coupling turned off, i.e., with $Q_0 = 0$. The irregular solutions agreed with pure Coulomb functions to within a few tenths of a percent. The uncoupled regular solutions, which should be exponentially decreasing going into the barrier, were not stable inside the barrier, but they were smaller than the irregular solutions by a factor of approximately 10^5 , which is more than sufficiently accurate for this problem. The radial integration interval was varied by an order of magnitude to insure that accuracy was not limited by choice of mesh size.

In order to check the completeness and accuracy of the quadrupole coupling matrix elements, the rotational energy and the centrifugal energy of each group were set equal to zero. The regular Coulomb function $F_0(\eta, \rho)$ with η and ρ appropriate for the $I_d = 7/2$ channel was integrated inward from 150 fm with $Q_0 = 13.1$ b. The d and the g waves were found to branch in the ratio of Clebsch-Gordan coefficients as they should.

A relative penetrability can be approximated by the ratio of the uncoupled regular function at 10 fm to the uncoupled regular function at 150 fm squared. Each squared ratio was divided by the corresponding penetrability given by Poggenburg,¹¹ who used a Fröman matrix to calculate penetrabilities. The resulting quotients should be, and were, approximately equal.

Acknowledgment

This work was supported by the U.S. Energy Research and Development Administration. We wish to acknowledge helpful comments from Richard Chasman. We are grateful to Irshad Ahmad for encouragement and for sending us his data in advance of publication.

References

1. R. R. Chasman and J. O. Rasmussen Phys. Rev. 115 (1959) 1257.
2. I. Ahmad, F. T. Porter, M. S. Freedman, R. F. Barnes, R. K. Sjoblom, Phys. Rev. C2 (1971) 390. I. Ahmad and J. Milsted, Nucl. Phys. A239 (1975) 1.
3. A. J. Soinski, R. B. Fränkel, Q. O. Navarro and D. A. Shirley, Phys. Rev. C2 (1970) 2379.
4. A. Bohr, P. O. Fröman, and B. R. Mottleson, Kgl. Danske Videnskab. Selskab, Mat.-Fys. Medd 29, No. 10 (1975).
5. I. Perlman and J. O. Rasmussen, Handbuch der Physik, ed. S. Flügge (Springer Verlag, Berlin) Vol. 42 (1957) 169.
6. Z. Szymanski, S. Wycech, C. Gustafson, I. Lamn, P. Moeller and B. Nilsson, Nucl. Phys. A131 (1969) 1.
7. H. C. Pauli, Phys. Rep. 7C (1973) 35.
8. J. O. Rasmussen in Alpha-, Beta-, and Gamma-Ray Spectroscopy, edited by K. Siegbahn (North-Holland Publishing Company, Amsterdam, The Netherlands, 1965), Vol. 1, p. 701.
9. M. Abramowitz in Handbook of Mathematical Functions, edited by M. Abramowitz and I. A. Stegun (National Bureau of Standards, Washington, D.C., 1964), p. 537 and C. Fröberg, Rev. Mod. Phys. 27 (1955) 399.
10. T. Tamura, Rev. Mod. Phys. 37 (1965) 679.
11. E. A. Rauscher, J. O. Rasmussen, and K. Harada, Nuc. Phys. A94 (1967) 33.
12. A. J. Soinski, Thesis, Lawrence Berkeley Laboratory Report, LBL-3411, September, 1974 (unpublished).

13. A. J. Soinski, E. A. Rauscher, J. O. Rasmussen and D. G. Raich, LBL Nuclear Science Annual Report, LBL-5057 (1975) 296.
14. J. O. Rasmussen and E. R. Hansen, Phys. Rev. 109 (1956) 1656.
15. A. Bohr and B. R. Mottelson, Kgl. Danske Videnskab. Selskab, Mat.-Fys. Medd. 22, No. 16 (1953).
16. F. Asaro, S. G. Thompson, F. S. Stephens and I. Perlman, Proceedings of the International Conference on Nuclear Structure, Kingston, edited by D. A. Bromley and E. W. Vogt (University of Toronto Press, Toronto, Canada, 1960) p. 581.
17. Y. A. Ellis and M. R. Schmorak, Nucl. Data Sheets 8 (1972) 345.
18. J. K. Poggenberg, Thesis, Lawrence Berkeley Laboratory Report, UCRL-16187, August 1975 (unpublished).
19. J. K. Poggenburg, H. J. Mang and J. O. Rasmussen, Phys. Rev. 181 (1969) 1697.
20. P. O. Fröman, Kgl. Danske Videnskab. Selskab. Mat.-Fys. Medd. Skrifter 1, No. 3 (1957).
21. L. A. Malov and V. G. Soloviev, Sov. J. Nucl. Phys. 5 (1967) 403.
22. F. A. Gareev, S. P. Ivanova, L. A. Malov and S. G. Soloviev, Nucl. Phys. A171 (1971) 134.
23. I. Ahmad, Private Communication, 1974.

Figure Legends

- Fig. 1 Ratio of the hindrance factor of the second excited level to that of the first excited level in the favored alpha decay band of odd-mass nuclei.¹⁷
- Fig. 2 Favored band alpha branching calculations for ^{253}Es compared with experiment (arrows). The left-hand bars represent coupled-channel, logarithmic least squares fits with the constraint $m_\ell = 0$. The right-hand bars are fits with an additional parameter, the tilt angle θ , varied, (see text).
- Fig. 3 Same as Fig. 2 except for ^{255}Fm .
- Fig. 4 Logarithm of the calculated ratios of $\ell = 4$ partial waves as a function of α_4 , with α_2 fixed at 0.89. The coupled channel calculations are for ^{253}Es with $m_\ell = 0$ constraint. The BFM ratios (Clebsch-Gordan coefficients squared) are shown at the left.

Table I. ²⁵³Es partial wave intensities, quadrupole phase shifts, and Coulomb phase shifts obtained by numerical integration ($\alpha_0 = 1$, $\alpha_2 = 0.8580$, $\alpha_4 = -0.0977$).

I_d	ℓ	Partial wave intensity (%)	Experimental intensity with i-wave subtracted (%)	Quadrupole phase shift (radians)	Coulomb phase shift (radians)
7/2	0	81.7983	90	-0.021	50.802
	2	8.9034		-0.130	53.816
	4	$\frac{0.1355}{90.8372}$		0.127	56.659
9/2	2	5.2180	6.6	-0.159	54.047
	4	$\frac{0.3383}{5.5564}$		0.138	56.891
11/2	2	0.7788	0.846	-0.193	54.338
	4	$\frac{0.2723}{1.0511}$		0.151	57.183
13/2	4	0.0848	0.0810	0.167	57.537
15/2	4	0.0085	0.011	0.184	57.963

Table II. ^{255}Fm partial wave intensities, quadrupole phase shifts and Coulomb phase shifts obtained by numerical integration ($\alpha_0 = 1$, $\alpha_2 = 0.7918$, $\alpha_4 = -0.1794$).

I_d	ℓ	Partial wave intensity	Experimental intensity with i-wave subtracted (%)	Quadrupole phase shift (radians)	Coulomb phase shift (radians)
7/2	0	86.1522	93.4	-0.007	49.495
	2	7.5837		-0.136	52.505
	4	$\frac{0.2035}{93.9393}$		0.110	55.343
9/2	2	3.9054	5.05	-0.179	52.807
	4	$\frac{0.4433}{4.34487}$		0.122	55.646
11/2	2	0.5004	0.62	-0.226	53.180
	4	$\frac{0.3013}{0.8017}$		0.134	56.021
13/2	4	0.0787	0.097	0.146	56.471
15/2	4	0.0066	0.008	0.158	56.994

Table III. Comparison among theories of calculated branching ratios for the $\ell = 4$ groups from ^{253}Es .

I_d	BFM-sharp barrier (Asaro <i>et al.</i>) ¹⁶	BFM-sloping barrier (Poggenburg) ¹⁷	Coupled-channel (this work)
7/2	(1)	(1)	(1)
9/2	2.57	2.486	2.499
11/2	2.10	1.994	2.010
13/2	0.65	0.632	0.626
15/2	0.065	0.063	0.063

Table IV. Correction factors for the i partial wave.

$I_{d\pi}$	^{253}Es		^{255}Fm	
	Experimental intensity ³⁸ (%)	$\ell = 6$ component (%)	Experimental intensity ³⁸ (%)	$\ell = 6$ component (%)
7/2+	90.0(5)	0.0002	93.4(2)	0.0003
9/2+	6.6(2)	0.0014	5.05(7)	0.0022
11/2+	0.85(3)	0.0037	0.62(1)	0.0040
13/2+	0.085(3)	0.0039	0.110(5)	0.0129
15/2+	0.013(1)	0.0018	0.013(2)	0.0049
17/2+	0.0004(1)	(0.0004)		
19/2+	0.00012(4)			

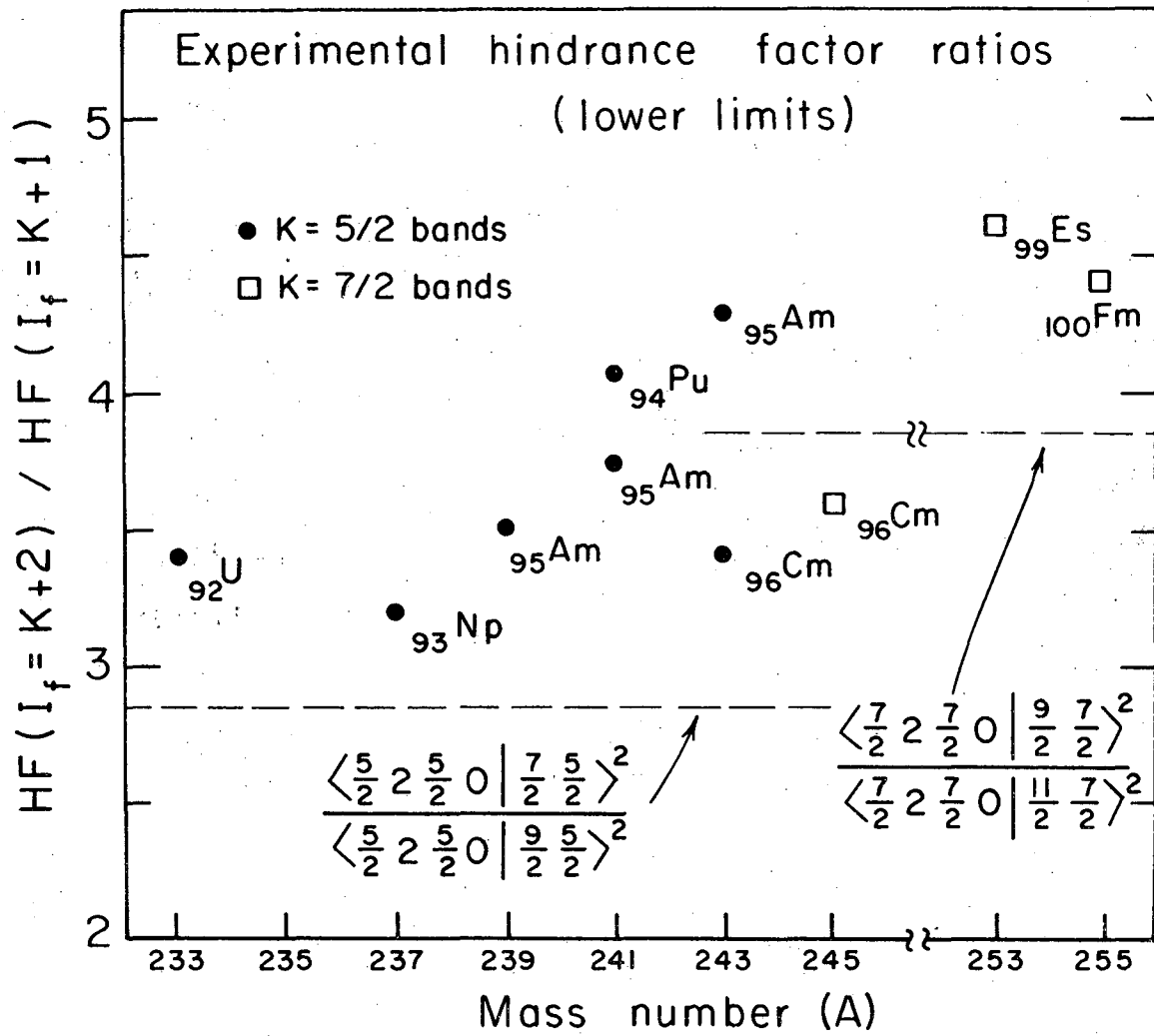
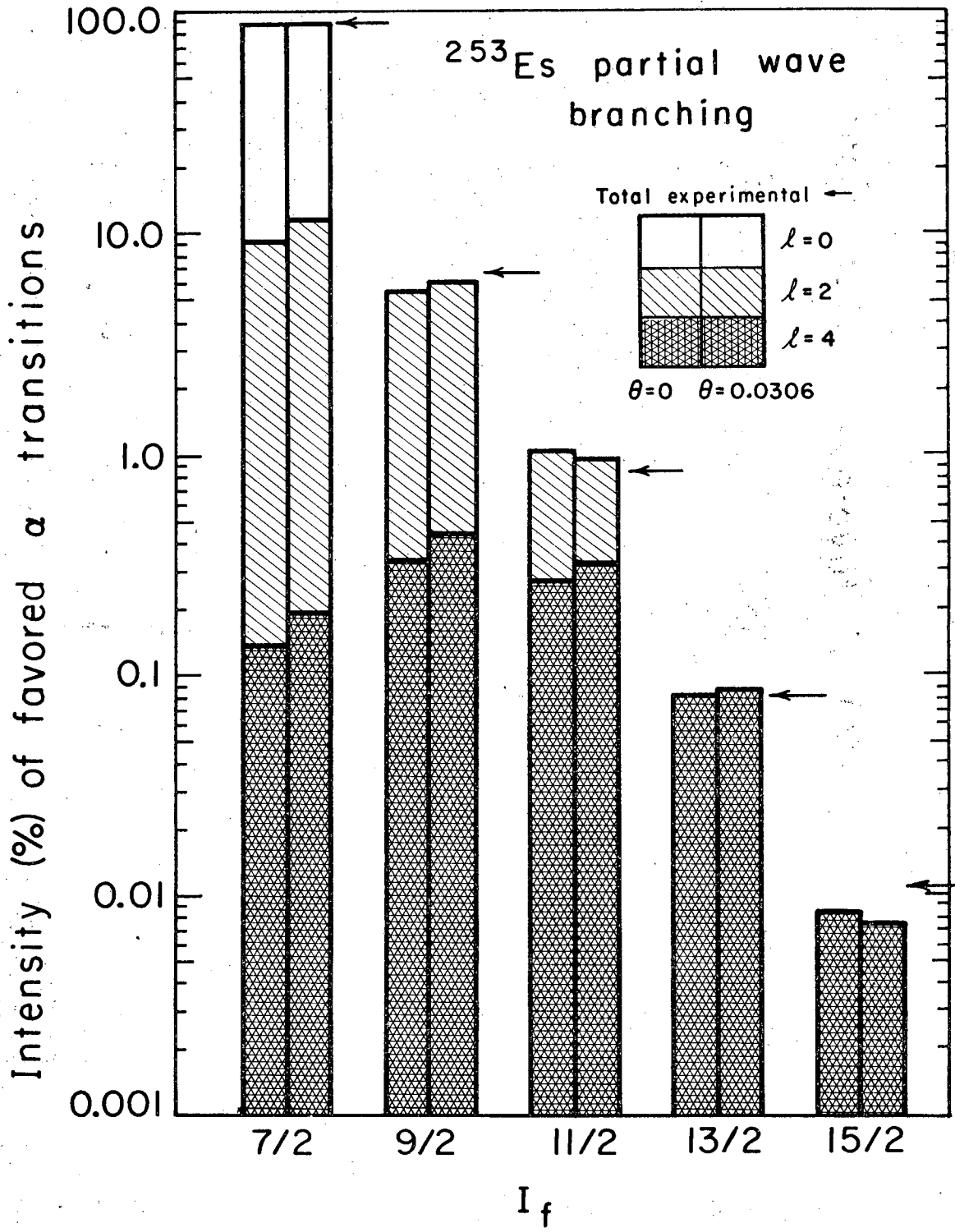
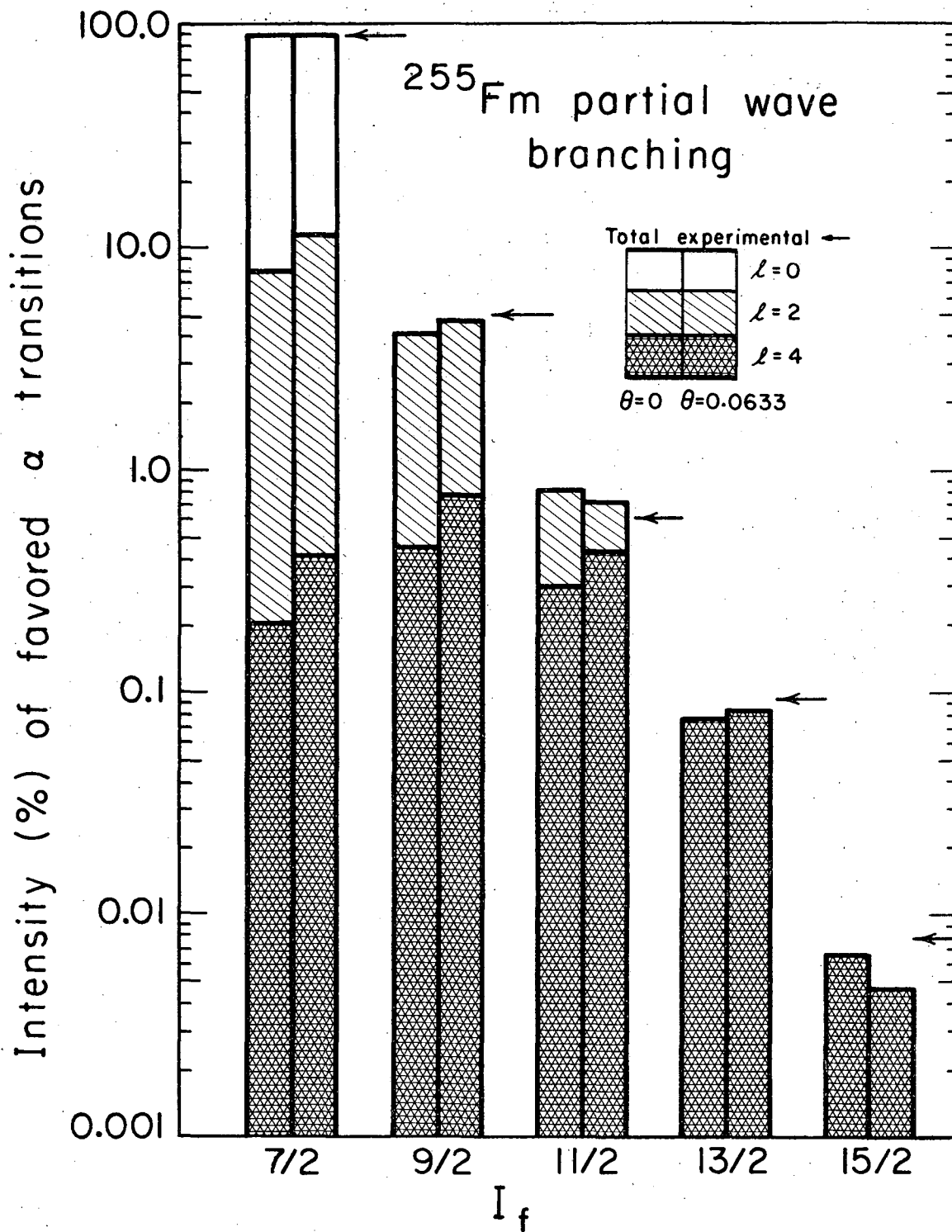


Fig. 1



XBL743-2687

Fig. 2



XBL743 - 2686

Fig. 3

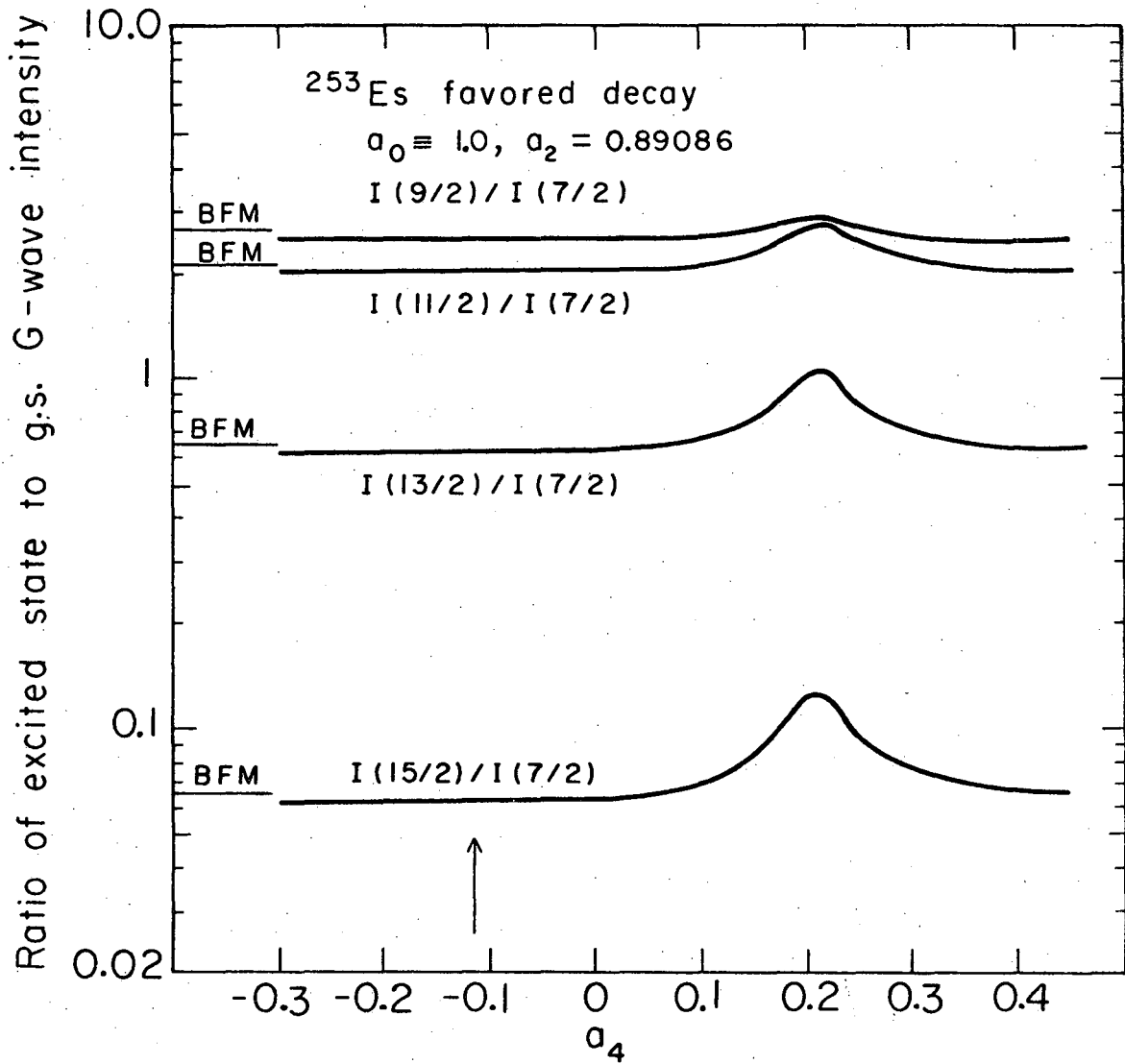


Fig. 4

This report was done with support from the United States Energy Research and Development Administration. Any conclusions or opinions expressed in this report represent solely those of the author(s) and not necessarily those of The Regents of the University of California, the Lawrence Berkeley Laboratory or the United States Energy Research and Development Administration.

TECHNICAL INFORMATION DIVISION
LAWRENCE BERKELEY LABORATORY
UNIVERSITY OF CALIFORNIA
BERKELEY, CALIFORNIA 94720